Proceedings of ASME TURBO EXPO 2004:
Power for Land, Sea and
June 14-17, 2004- Vienna, Austria

GT2004-53572

Evaluation of Predicted Heat Transfer on a Transonic Blade Using v^2 -*f* Models

Ali A. Ameri
Senior Research Associate
U. of Toledo/ NASA Glenn Research Center
Cleveland, Ohio U.S.A.

Kumud Ajmani
Senior Engineer
Tai-Tech Inc.
NASA Glenn Research Center
Cleveland, Ohio U.S.A.

ABSTRACT

The $v^2 - f$ models of Durbin and the new $v^2 - f$ model of Jones et al. were used to compute the blade heat transfer for the transonic cascade of Giel et al.. Three different experimental cases were considered. Calculations were performed using the Glenn-HT code modified so that it solves these turbulence model equations using an implicit scheme. An iterative matrix solver, namely GMRES was used for this purpose. Comparisons were made with previously published results using the SST model and a simple algebraic model modified for the stagnation heat transfer effects and transition effects. The results, albeit limited to the present case, show that the $v^2 - f$ model of Durbin provides good predictions on the pressure surface. But there is some discrepancy between the suction surface heat transfer predictions and experimental measurements. The newer model of Jones et al. requires further modification before it can be routinely used for blade heat transfer.

INTRODUCTION

The most common means of modeling turbulence in CFD codes today is the use of two equation eddy viscosity models. The k-ε and k-ω models are the most frequently used models of this type. Turbulence modeling is commonly faulted as the cause of deviations from measured data in the prediction of blade heat transfer. Turbulence models are designed to predict shear flows and often do predict the correct level of heat transfer for such flows. Prediction of blade heat transfer however includes prediction of heat transfer in the stagnation as well as end wall; near end wall; near the tip and the tip heat transfer. This involves complex flow fields, which are different from the simpler shear flows. In two papers, Medic and Durbin [1,2] showed the ability of the $v^2 - f$ model to produce accurate heat transfer predictions with and without the presence of film cooling. They also put forth modifications to two-equation models, which, if implemented, would help improve heat transfer predictions in the stagnation region. The necessity for such modifications comes from the fact that two-equation models over-estimate the stagnation flow turbulent energy leading to an over-estimation of the stagnation heat transfer. This, they suggest, could be due to one of two causes; an under-estimation of the turbulent dissipation, or the over-estimation of eddy-viscosity in the stagnation region.

One difficulty with the $v^2 - f$ model has been the stiffness of the equations and difficulty of convergence. This has been addressed by Lien and Durbin [3] by modifying the equations for $\overline{v^2}$ and f so that the boundary condition on f changed from depending on the other variables to being trivial. Another approach was taken by Jones et al. [4] to improve the robustness of the $v^2 - f$ model. This approach was to maintain the philosophy of the formulation but to use ω instead of ε, which is known to be non-singular near walls. We have not used Lien and Durbin's modification in our work because we were able to obtain converged solutions for the cases we considered by using an implicit solution method. However, we have included the model of Jones et al. [4] in our computations and will show comparisons with predictions of the original $v^2 - f$ model.

More sophisticated models, which do not use the eddy viscosity hypothesis and directly model the Reynolds stresses, are good candidates for use as well. Unfortunately, these models, which solve transport equations for Reynolds stresses and an equation for ε ,are CPU-time consuming, and difficult to converge. In recent years, a new Reynolds stress model, called Stress-ω, which is based on ω equation in place of ε, has been devised by Wilcox [5] with very good numerical properties.

The various versions of $v^2 - f$ model and the Stress-ω model have been implemented into the Glenn-HT code [6] and have been used to calculate the rate of blade heat transfer for the transonic cascade of Giel et al. [7]. We will show results of our calculations with emphasis placed on the $v^2 - f$ models. We will also compare the present results with the calculations of Garg and Ameri [8] (which use the Shear Stress Transport (SST) model of Menter [9]), and those of Giel et al. [7] (which were obtained using an algebraic (zero equation) model). A single comparison with the stress-ω Reynolds stress model will also be presented.

The literature contains a reference to Kalitzin and Iaccarino[10] who have performed heat transfer calculations on the endwall of the blade cascade considered in this paper. The results to be presented in this paper are only of the heat transfer on the blades and not on the endwall. This is because the experimental conditions imposed on the boundaries for the blade heat transfer and endwall heat transfer were different. As such, a comparison with the endwall heat transfer results requires would require a different set of computations.

NOMENCLATURE

- C_p specific heat
- D leading edge circle diameter
- f variable related to turbulence energy redistribution
- Fr $1/\sqrt{\mathrm{Re}_D}(hD/k)$
- h heat transfer coefficient $q_w/(T_w-T_{aw})$
- k turbulent kinetic energy, also thermal conductivity
- M Mach number
- P_k turbulence production from (3)
- Pr Prandtl number
- Re Reynolds number
- r recovery factor= $\mathrm{Pr}^{1/3}$
- St Stanton number, equation 13
- U magnitude of velocity
- V reference velocity (inlet)
- $\overline{v^2}$ velocity scale for turbulent transport
- y distance to the nearest wall

Greek Symbols

- δ inlet boundary layer thickness
- ε dissipation rate of turbulence
- γ specific heat ratio
- ν fluid kinematic viscosity
- ρ fluid density
- ω specific dissipation rate

Subscripts

- aw adiabatic wall value
- ex exit value
- in inlet value
- is isentropic value
- o stagnation value
- t turbulent value
- w wall value

FORMULATION OF THE TURBULENCE MODELS

Formulations of the SST model and the algebraic model have been given by Garg and Ameri [8] and Giel et al.[7] along with the results to which we will be referring. The equations for the Stress-ω model are given in Wilcox [5]. Formulations of two versions of the $v^2 - f$ model will be repeated here following Behnia et al. [11] and Medic and Durbin [1, 2]. The versions are very similar, and differ only in definition of some of the constants. One important difference is that one version uses the distance to the wall and the other version does not use the distance to the wall. In addition, the $k-\omega$ version of the $v^2 - f$ model hereafter referred to as $v^2 - f$ - $k-\omega$ model of Jones et al. [12] will also be repeated here.

v^2-f Model: This model is a simplification of the Elliptic Relaxation Reynolds Stress model of Durbin [13]. The simplified model requires the solution of three transport and one elliptic (relaxation) equation. The system of the Reynolds stress equations is replaced by a transport equation for a velocity scalar ($\overline{v^2}$) and an elliptic equation (for *f*). In the case of the full Reynolds stress model f_{ij}, would simulate the effect of the walls on the Reynolds stress components $\overline{v_i v_j}$. The equations for turbulent kinetic energy and the dissipation rate are:

$$\partial_t(\rho k) + \nabla.(\rho U k) = \rho P_k - \rho\varepsilon + \nabla.((\mu+\mu_t)\nabla k) \quad (1)$$

$$\partial_t(\rho\varepsilon) + \nabla.(\rho U\varepsilon) = \frac{C_{\varepsilon 1}\rho P_k - C_{\varepsilon 2}\rho\varepsilon}{T} + \nabla.((\mu + \frac{\mu_t}{\sigma_\varepsilon})\nabla\varepsilon) \quad (2)$$

In the above

$$\rho P_k = -\frac{2}{3}\rho k(\nabla.U) + 2\mu_t\,|S|^2 - \frac{2}{3}\mu_t(\nabla.U)^2 \quad (3)$$

where $|S|^2 = S_{ij}S_{ij}$ with $S_{ij} = 1/2(U_{i,j} + U_{j,i})$ and the turbulence time scale $T = k/\varepsilon$ is modified near the walls. Upon exerting realizibility constraint for the stagnation flow region, the time scale becomes:

$$T = \min[\max[\frac{k}{\varepsilon}, 6\sqrt{\frac{\nu}{\varepsilon}}], \frac{\alpha k}{\sqrt{3}\bar{v}^2 C_\mu\,|S|}] \quad (4)$$

Eddy viscosity is computed from the following:

$$\mu_t = C_\mu \rho \bar{v}^2 T \quad (5)$$

The constants are $C_{\varepsilon 1} = 1.3 + 0.25/[1.+(y/2L)^2]^4$ for the original version (hereafter called V1) which uses distance to the walls and $C_{\varepsilon 1} = 1.4(1.+0.046\sqrt{k/\bar{v}^2})$ for version 2 (V2) which does not use the distance to the walls. Other constants are; $C_{\varepsilon 2} = 1.92$, $C_\mu = 0.19$, $\sigma_\varepsilon = 1.3$, $\alpha = 0.6$.

The equation for $\bar{v}^2$ is given as:

$$\partial_t(\rho\bar{v}^2) + \nabla.(\rho U\bar{v}^2) = \rho k f - \rho\frac{\bar{v}^2}{k}\varepsilon + \nabla.((\mu+\mu_t)\nabla\bar{v}^2) \quad (6)$$

f, which represent a relaxation parameter that brings the effect of the walls into the equations, follows the elliptic equation:

$$f - L^2\nabla^2 f = (C_1 - 1)\frac{2/3 - \bar{v}^2/k}{T} + C_2\frac{P_k}{k} \qquad (7)$$

The following expression for the turbulent length scale applies:

$$L = \min[C_L \max[\frac{k^{3/2}}{\varepsilon}, C_\eta(\frac{\nu^3}{\varepsilon})^{1/4}], \frac{1}{\sqrt{6}}\frac{k^{3/2}}{C_\mu \bar{v}^2\sqrt{S^2}}] \qquad (8)$$

Values of other constants used above are: $C_L = 0.3$, $C_\eta = 70$ (for version 1) and $C_L = 0.23$ and $C_\eta = 85$ (for version 2). Also $C_1 = 1.4$ and $C_2 = 0.3$.

Wall boundary conditions: For solid walls with y denoting the distance to the wall of the first cell center, we have

$$k = \bar{v}^2 = 0., \varepsilon_w \rightarrow \frac{2\nu k}{y^2} \text{ and } f_w \rightarrow \frac{-20\nu^2\bar{v}^2}{\varepsilon y^4} \qquad (9)$$

v^2-*f*-*k*-ω model of Jones et al. Jones, Acharya and Harvey [4] recast the formulation of $v^2 - f$ model, basing it on ω instead of ε, in order to increase the robustness of the model. The following equation for ω was used.

$$\partial_t(\rho\omega) + \nabla.(\rho U\omega) = \alpha\frac{\omega}{k}P - \beta\omega^2(\frac{\bar{v}^2}{k})^{1-n} + \nabla.((\mu + \frac{\mu_t}{\sigma_\omega})\nabla\omega) \qquad (10)$$

The following relationship was proposed by Jones et al. between ω and ε

$$\varepsilon = func[\beta^*\omega k\overline{v^2}^{1-n}] + (1 - func)\frac{2\nu k}{y^2} \qquad (11)$$

where

$$func = [1 - e^{-0.02\mathrm{Re}_y}]^2 \text{ and } \mathrm{Re}_y = \frac{\sqrt{k}\,y}{\nu}$$

Jones et al. [4] found a value of $n = 0.7$ to give the best results for the cases they considered. Here eddy viscosity is defined using equation (5) and the other coefficients are:

$$\beta^* = 0.09, \beta = \frac{4}{5}\beta^*,$$

$C_1 = 0.4, C_2 = 0.3, \sigma_\omega = 1.5, C_L = 0.23$, C_μ =0.25 and

$$\alpha = \frac{\beta}{\beta^*} - \frac{1}{\sigma_\omega}[\kappa^2/\sqrt{\beta^*}]$$

Wall boundary conditions:

$$k = \bar{v}^2 = 0., \omega_w \rightarrow \frac{2\nu}{\beta^* y^2}\left(\frac{k}{\overline{v^2}}\right)^{1-n} \text{ and}$$

$$f_w \rightarrow \frac{-20\nu^2\bar{v}^2}{\varepsilon_w y^4}$$

Transition modeling

With the exception of Giel et al. [7] who included a transition model with their algebraic turbulence model, none of the other models has physically-based transition modeling incorporated in them. This is an important consideration affecting the heat transfer solution, as we will see later in the results section.

COMPUTATIONAL METHOD

The simulations in this study were performed using a multi-block computer code called Glenn -HT [6]. This code is a general-purpose flow solver designed for simulations of flows in complicated geometries. The code solves the full compressible Reynolds averaged, Navier-Stokes equations using a multi-stage Runge-Kutta based multigrid method. It uses the finite volume method to discretize the equations. The code uses central differencing together with artificial dissipation to discretize the convective terms. The overall accuracy of the code is second order. For heat transfer, unless the Reynolds stress model is used, a constant value of 0.9 for turbulent Prandtl number Pr_t is assumed. Viscosity is a function of temperature through a 0.7 power law (Schlichting [14]) and C_p is taken to be a constant. In the case of a Reynolds stress model, the Generalized Gradient Diffusion Hypothesis (GGDH) (given in for example Iacovides et al. [15]) was used.

The k-ω model and Stress-ω model lend themselves nicely to solution by explicit schemes, although pointwise coupling of the equations may be necessary. However, our basic explicit solution methodology proved to be ineffective for solving the $v^2 - f$ model equations. Therefore, the turbulence equations were discretized and written in an implicit form and solved using an iterative matrix solver algorithm namely, GMRES (Wington et al. [16]). The k - ε equations and $\bar{v}^2$ and f were coupled in pairs through their solid wall boundary conditions.

RESULTS

Grid and Geometry The blade for the transonic-blade cascade has an axial chord of 12.7 cm and has a pitch of 13 cm. The blade span is 15.24 cm. The inlet flow angle is 63.6 degrees and the design flow turning angle is 136 degrees. The blade was designed to yield a highly three-dimensional passage flow to be used for CFD validations. A multi-block grid similar in topology to the one shown in Fig. 1 was used for the calculations presented in this paper. The grid in Fig.1 has been coarsened for better visualization. The grid is only for half the span since a symmetry boundary condition was used at the mid span. The grid contains approximately 800,000 nodes and is refined near the walls to better capture the wall heat transfer. This is done by choosing the non-dimensional distance (y^+) to be near unity. There were 68 grid cells covering the hub to mid-span in the spanwise direction. The grid was used for the v^2 - f model and stress-ω model calculations. The primary reason for using a grid with so many nodes was the requirements placed on grid convergence by the Stress-ω Reynolds stress

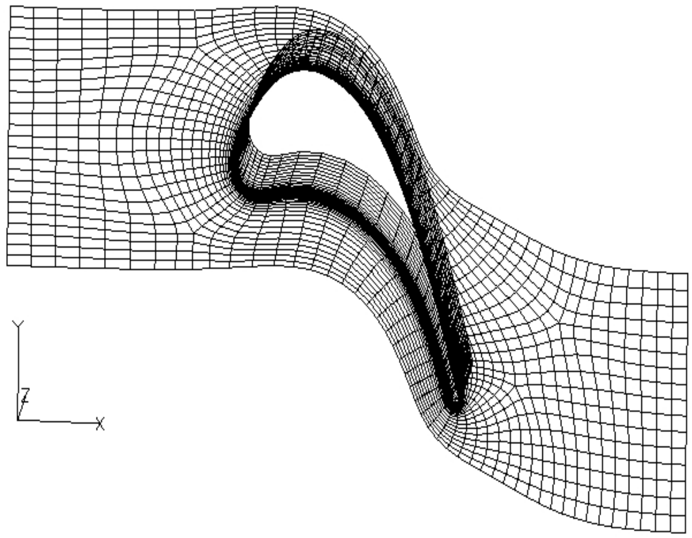

Fig.1 Grid for the hub and blade of the Transonic Cascade

model. This results in a grid for the $v^2 - f$ model calculations that is very fine. For comparison, the grid density found to provide grid convergence for the SST model and the algebraic model from [7] and [8] were 360,000 and 660,000 cells. The latter used 48 cells in the spanwise direction.

Flow Conditions

The experiment of Giel et al.'s [7] matrix of cases consists of eight combinations of independent variables. We only pick three of those conditions here for analysis. The cases considered all have an inlet Reynolds number of one million. Conditions are given in the table below:

Table 1: Run Conditions

Case	Re_{in}	M_{ex}	Tu_{in}	Length scale	Inlet δ, % of half span
1	10^6	0.98	0.09	0.23	26
2	10^6	0.98	0.0025	0.01	40
3	10^6	1.32	0.09	0.23	26

Heat Transfer

Figure 2(a) shows the experimentally obtained results for the blade heat transfer in case-1 of the above table. The data was obtained from a calibrated resistance layer in conjunction with a surface temperature measured by calibrated liquid crystals. Figure 2(b) show the calculation results using the $v^2 - f$ model for the blade surface. The abscissa is the wetted distance normalized by the axial chord. The wetted distance is measured from the geometric stagnation point. The ordinate is the normalized span. Heat transfer is plotted in terms of Stanton number defined as:

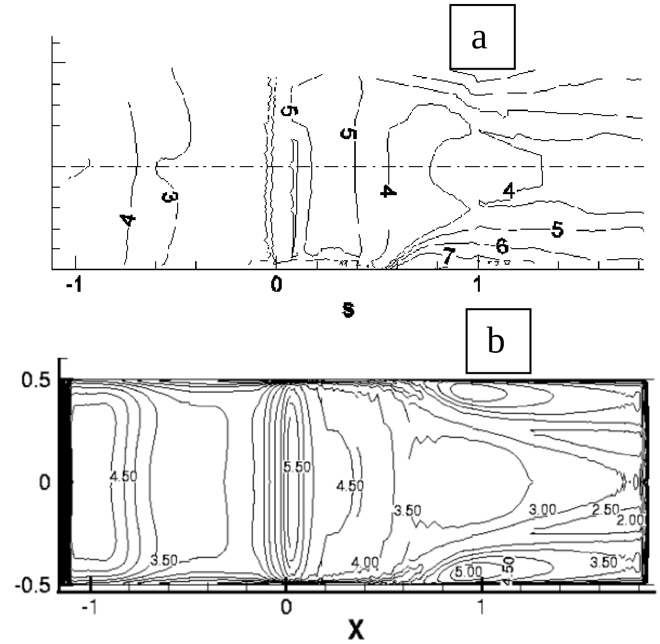

Fig. 2 Surface heat transfer in terms of Stantonx1000, for case 1 of Table 1, (a) from Giel et al.[3] and (b) predicted using $\overline{v^2}$ -*f* (version 2) model.

$$St = \frac{-(k\partial T/\partial y)_w}{\rho_{in} U_{in}\, C_p (T_w - T_{aw})} \tag{12}$$

Where the local adiabatic wall temperature, T_{aw} is

$$\frac{T_{aw}}{T_{0,in}} = r + \frac{1-r}{1+0.5(\gamma-1)M_{is}^2} \tag{13}$$

The figure shows that the heat transfer on the pressure side of the blade is quite two-dimensional. The distribution of the

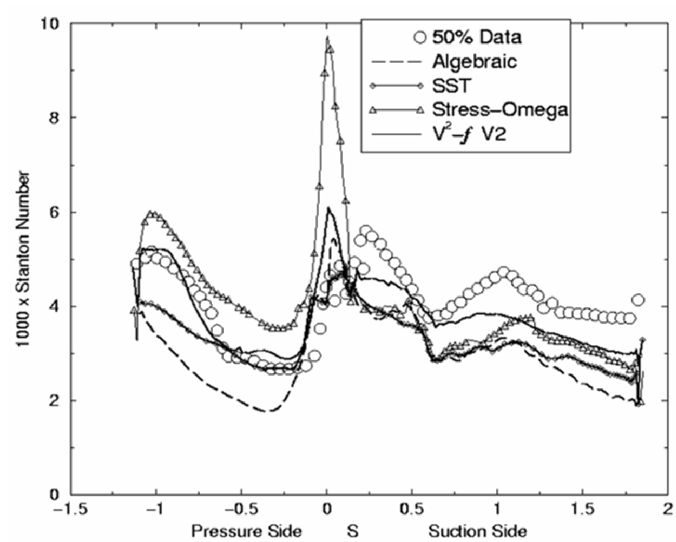

Fig. 3 Comparison of four turbulence models for the Transonic Blade at the mid span (Case 1)

heat transfer rate on the suction side however attests to the three-dimensionality of the flow. It is possible to distinguish the region of the blade dominated by the endwall secondary flow starting from the low pressure point on the suction side where the pressure side leg of the horseshoe vortex meets the adjacent blade. At this location, the level of heat transfer is quite elevated and according to the experiments of Giel et al. [7] reaches the highest level on the entire blade.

Figure 3 shows the mid span heat transfer results obtained for the transonic-blade with four turbulence models. The results were obtained using; an algebraic model, the Shear Stress Transport (SST) model of Menter [9], the Stress-ω model, and the v^2-f model. The algebraic model is that of Chima et al. [17] and the results are from Giel et al. [7]. The results of the algebraic model should be viewed as representing the particular model used by Giel et al. The SST model is an amalgam of the k-ω and the k-ε models. The former is activated in the near wall region and the latter in the outer wake and free shear layers. The SST model results are from Garg and Ameri [8].

It is obvious from Fig. 3 that the Stress-ω model over-predicts the heat transfer on the pressure side and greatly over-predicts the heat transfer in the stagnation region. This behavior has been addressed by Durbin [18] where he referred to this phenomenon as the "stagnation point anomaly." The fact that the Stress-ω model also suffers from the stagnation point anomaly was initially a surprise. Surveying the literature, it becomes apparent that this has been, and currently is a research problem concerning Reynolds stress models [19]. Use of the remedies suggested by Medic and Durbin do improve the stagnation point heat transfer but cause a further deterioration of the prediction on the rest of the blade. In light of these issues, no further calculations with the stress-ω model were made.

In summary, Fig. 3 shows that, the $v^2 - f$ model performs reasonably well and that further investigation is justified.

Figure 4 shows the comparisons for case 1 of Table 1. The top figure shows comparisons for the 50% (mid) span while the middle and the bottom graphs show comparisons of 25% and 10% span. Both versions of the $v^2 - f$ model are used and shown here. As explained earlier, version-1 uses the distance to the wall while version-2, does not. There is some difference between the predictions from the two models. Version-1 provides a prediction that is superior to that of version-2, especially on the pressure side. The SST model also does well on the pressure side. The algebraic model's prediction of heat transfer on the pressure side is too low. In the near leading edge of the suction side, at 50% span, $v^2 - f$ models appear to do better than the SST model and the algebraic model. For the 25% and 10% span, the $v^2 - f$ model does not provide a good prediction on the suction side. This is because the level of heat transfer on the low pressure area on the suction side is underpredicted (Fig. 2). For the 25% and 10% span locations, the algebraic model provides better predictions than the $v^2 - f$ models on the suction side.

In Fig. 5 results of the application of the $v^2 - f$ to case-2 (Table 1) are shown. This case has a lower incoming turbulence intensity and a much thinner incoming boundary layer

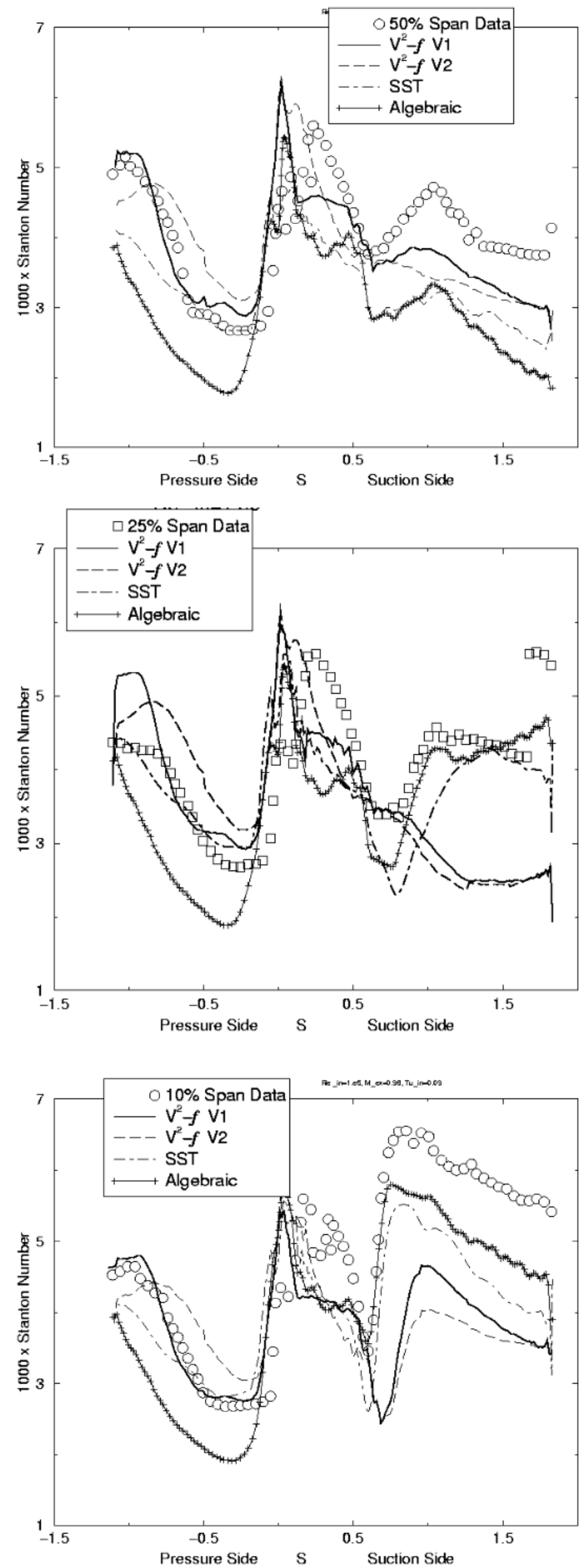

Fig. 4 Prediction of heat transfer for Case 1 using the two versions of the $v^2 - f$ model and comparison with the SST model from Garg and Ameri[8] and Algebraic model from Giel et al. [7]

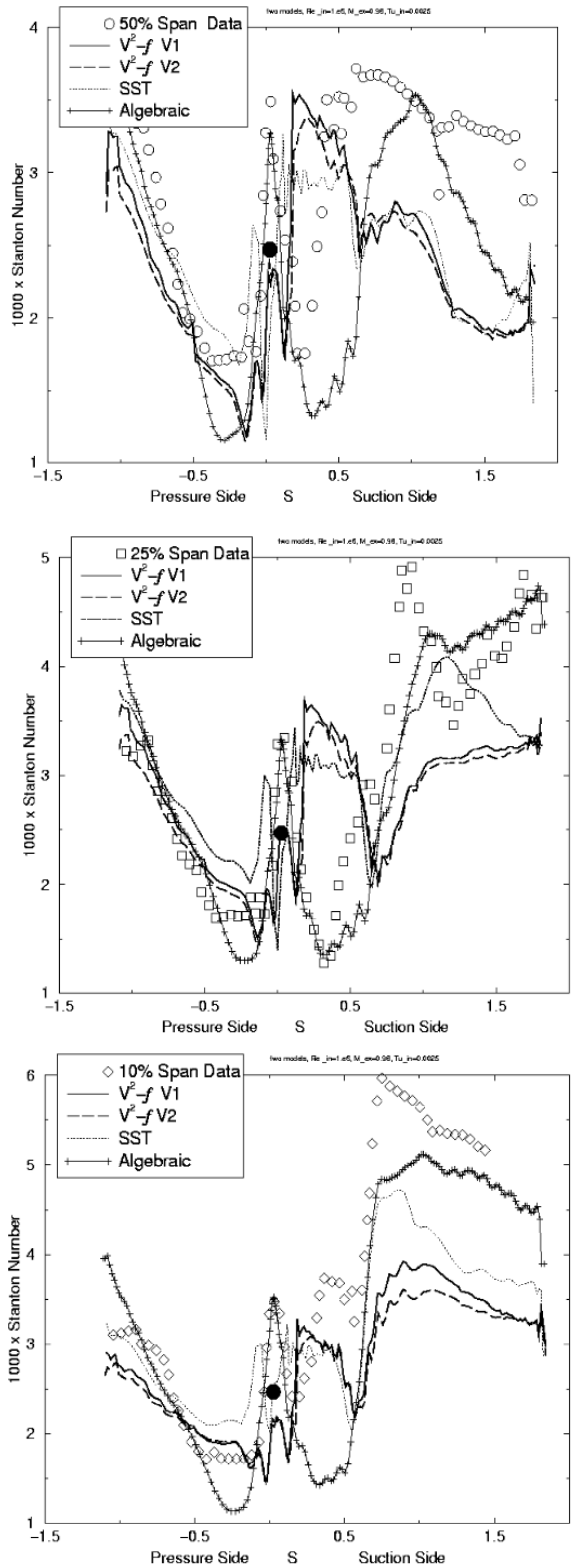

Fig.5 Prediction of heat transfer for Case 1 using the two versions of the $v^2 - f$ model and comparison with the SST model from Garg and Ameri [8] and Algebraic model from Giel et al. [7]. Corrected stagnation value is shown with ●

compared to case-1. The calculated stagnation values appear to

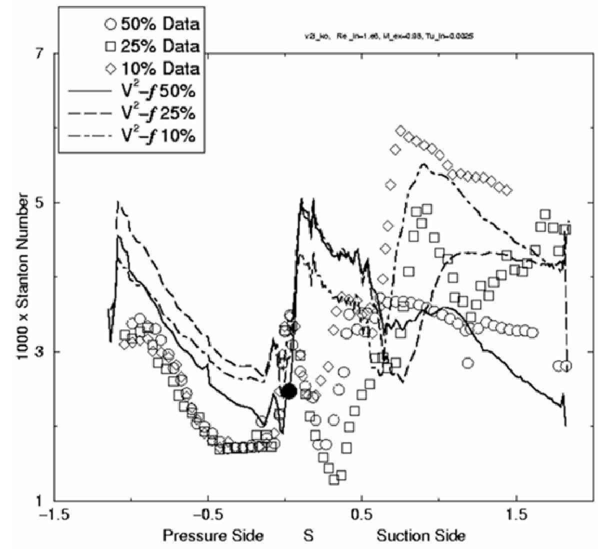

Fig. 6 Calculations with v^2–f–k–ω model of Jones et al. [4] for case 2. Corrected stagnation value is shown with ●

be too low. Note that the approaching flow is quite calm and the turbulence intensity is very low. For laminar flows, as this flow should be around the leading edge, the heat transfer results should have been better predicted.

In a recent paper, Boyle et al.[20] have reported their findings regarding the stagnation data for this case. They calculated the Frossling (*Fr*) number from the measured data to be 1.4. In reality, *Fr* should be near unity given the state of the incoming flow. That would correct the Stanton number to the value shown as a dark circle on Fig. 5, which would a better match with the predictions.

Agreement on the pressure side is quite good at all three locations. The suction side heat transfer only qualitatively agrees with the calculated data for the mid span. When using the $v^2 - f$ and SST models the transition starts too early. With the algebraic model, the transition starts somewhat downstream of the location suggested by the experimental data. Overall, the algebraic model provides the best agreement. Even though we do not expect to find a case with such low turbulence intensity upstream of the blade in practice, the sensitivity of the models to the level of turbulence is encouraging.

Figure 6 presents the results using the $v^2 - f - k - \omega$ model. On the suction side,the flow apparently is fully turbulent immediately past the stagnation region. This is in contrast to the experimental data, which clearly shows a laminar region in the leading part of the blade. Agreement with the data is good past the transition location for all spanwise locations, but the agreement for the pressure side and the leading edge region is not very satisfactory.

Figure 7 shows the results for the case 3 (Table 1), namely high turbulence intensity and higher exit Mach number. This case is especially interesting because of the existence of the reflected shock on the suction side downstream of the throat. The pressure side heat transfer predictions agree with the data, with the exception of the algebraic model. The mid span heat transfer on the suction side is predicted best with the $v^2 - f$

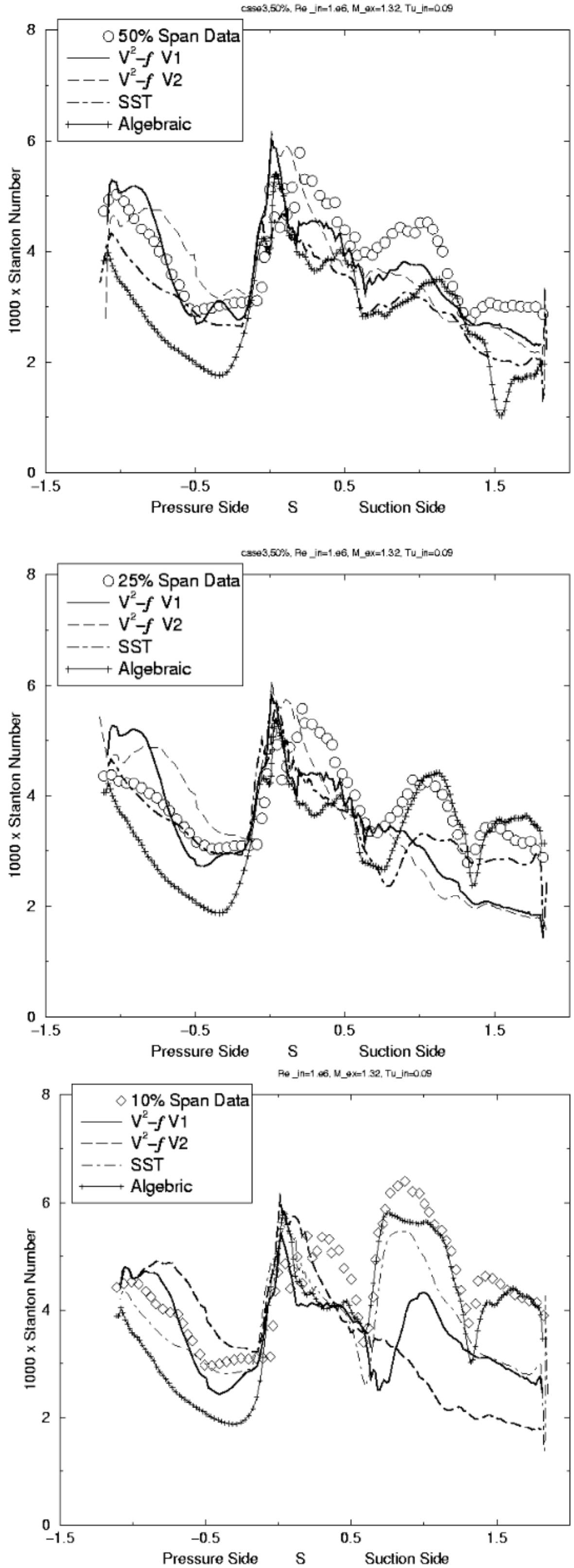

Fig. 7 Prediction of heat transfer for Case 3 using the two versions of the $v^2 - f$ model and comparison with SST model from Garg Ameri [8] and algebraic model from Giel et al. [7]

model. At the other two spanwise locations, the $v^2 - f$ model

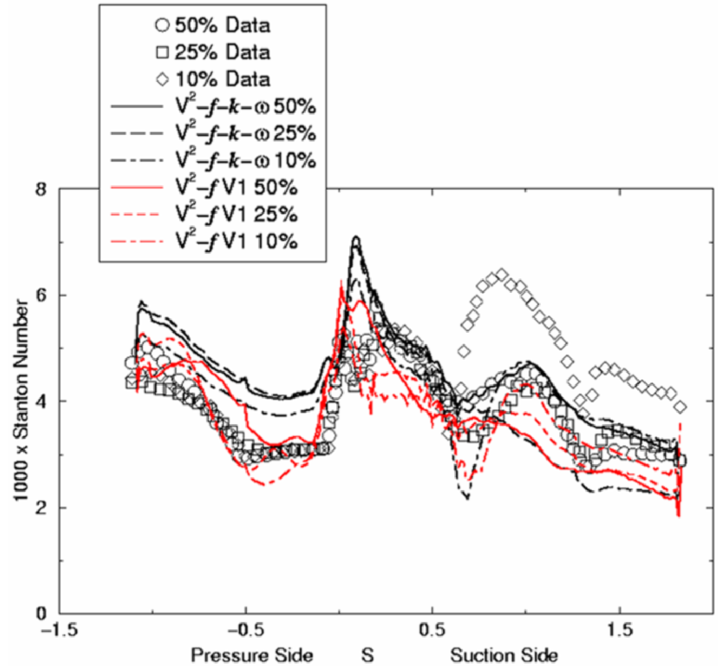

Fig. 8 Prediction of heat transfer for Case 3 using the two the v^2-f-k-ω model of Jones et al. [4]

is inferior to the algebraic model and fares worse than the SST model on the pressure side. In fact, the variation due to the shock boundary layer interaction is, for the most part, missed by all the models, except for the algebraic model.

Figure 8 shows the prediction as obtained using the $v^2 - f - k - \omega$ model with comparison to version-1 of the $v^2 - f$ model. The pressure side and the stagnation region heat transfer are over-predicted. Agreement for the mid span heat transfer is quite good, but the increase in the rate of heat transfer due to the secondary flow near the endwall is not captured. Again, the effect of the reflected shock on the suction side is not captured.

CONCLUSIONS

The transonic-blade data of Giel et al. [7] was used to test some of the various versions of the $v^2 - f$ model available to date. The results obtained using Durbin's $v^2 - f$ show some improvement over the other models but the overall improvement in the heat transfer predictions was found to be modest. Specifically, the improvements included the consistently good pressure side predictions and improved predictions of the heat transfer on the suction side immediately downstream of the stagnation region. For the suction side heat transfer, the $v^2 - f$ model did not fully capture the three-dimensional heat transfer effect on the blade. Specifically, the heat transfer rise due to the effect of the pressure side leg of the horseshoe vortex on the blade suction side and near the endwall was underpredicted. Overall, version-1 of the model (the original model) performed better than the version-2 model.

As for the $v^2 - f - k - \omega$ model, which was designed to be more robust numerically than the $v^2 - f$ models, it requires more refinement before it becomes a useful tool for predicting blade heat transfer.

ACKNOWLEDGMENTS

The authors wish to thank Dr. Raymond Gaugler, Chief of the Turbine Branch at NASA Glenn Research Center for his support of this work. Thanks are also due to our colleague Dr. Vijay K. Garg.

REFERENCES

[1] Medic, G. and Durbin, P.A., 2002, "Toward Improved Film Cooling Prediction," J. of Turbomachinery, Vol. 124, pp. 193-199.

[2] Medic, G. and Durbin, P.A., 2002, "Toward Improved Prediction of Heat Transfer on Turbine Blades," J. of Turbomachinery, Vol. 124, pp. 187-192.

[3] Lien, F. S., Durbin P. A. and Parneix, S. , 1996, "Non-Linear v^2-f Modeling with application to Aerodynamic Flows," Proc. of the summer program, Center for Turbulence Research, NASA Ames/Stanford Univ.

[4] Jones, R., Acharya, S., and Harvey, A., in Modeling and Simulation of Turbulent Heat Transfer, edited by Bengt Sunden and Mohammad Faghri, WIT Press, 2003

[5] Wilcox, D. C., 1998, Turbulence Modeling for CFD, Second Edition, DCW Industries, Inc. La Canada, CA.

[6] Steinthorsson, E., Liou, M.S., and Povinelli, L.A., 1993, "Development of an Explicit Multiblock/Multigrid Flow Solver for Viscous Flows in Complex Geometries," AIAA-93-2380.

[7] Giel, P. W., VanFossen, G. J., Boyle, R. J., Thurman, D. R, and Civinskas, K. C., "Blade Heat Transfer Measurements and Predictions in a Transonic Turbine Cascade", ASME 99-GT-125.

[8] Garg, V.K. and Ameri, Ali A., 2001, "Two-Equation Turbulence Models for Prediction of Heat Transfer on a Transonic Blade," Int. J. of heat and fluid flow, Vol. 22, 2001. pp. 593-602.

[9] Menter, Florian R., 1993, "Zonal Two-Equation k-ω Turbulence Models for Aerodynamic Flows," AIAA-93-2906.

[10] Kalitzin, Georgi and Iaccarino, Gianluca, 1999, "Endwall Heat Transfer Computations in a Transonic Turbine Cascade," 17th UIT National Heat Transfer Conference. Universita Degli Studi Di Ferrara.

[11] Behnia, M., Parneix, and Durbin, P. A., 1998, "Prediction of Heat Transfer in an Axisymmetric Impinging on a Flat Plate," Int. J. of Heat and Mass Transfer 41, 1845-1855.

[12] Jones, R., Acharya, S., and Harvey, A., "A new k-ω-v^2-f Model for Turbulent Flows," AIAA Journal, submitted for review.

[13] Durbin, P. A. and Pettersson Reif, B. A., Statistical Theory and Modeling for Turbulent Flows. John Wiley & Sons, LTD.

[14] Schlichting, H. Boundary Layer Theory. McGraw-Hill, New York, seventh ed. pp. 312-313.

[15] Iacovides, H., Launder, B. E. and Li, H.-Y., "Application of a Reflection-Free DSM to Turbulent Flow and Heat Transfer in a Square-Sectioned U-Bend," Experimental Thermal and Fluid Science 1996: 13:419-429.

[16] Wington, L.B., Yu, N.J. and Young, D. P., 1985, "GMRES Acceleration of Computational Fluid Dynamics Codes," AIAA paper 85-1494.

[17] Chima, R. V., Giel, P. W. and Boyle, R. J., 1993 "An Algebraic Turbulence Model for Three-Dimensional Viscous Flows", NASA TM-105931, presented at the 31st AIAA Aerospace Sciences Meeting, Reno, Nevada, January 11-14, 1993.

[18] Durbin, P. A., 1996, "On the $k-\varepsilon$ Stagnation Point Anomaly," Int. J. Heat and Fluid Flow, 17, pp. 89-90.

[19] Craft, T.J., Graham, L. J. W. and Launder, B. E.,1993, "Impingement Jet Studies for Turbulence Model Assessment-II. An Examination of the Performance of Four Turbulence Models," Int. J. Heat Mass Transfer, Vol. 36, No. 10, pp. 2685-2697.

[20] Boyle, R. J., Giel, Paul, W., and Bunker, Ronald S., 2003, "Predictions for the Effects of Turbulence on Turbine Blade Heat Transfer," AIAA paper, ISABE-2003-1178